V.G. LITOVCHENKO, V.P. MELNIK, B.M. ROMANJUK

V.E. Lashkaryov Institute of Semiconductor Physics, Nat. Acad. of Sci. of Ukraine
(41, Prosp. Nauky, Kyiv 03028, Ukraine)

NANO-SIZE PHASE FORMATION AT ACOUSTICALLY STIMULATED ION BEAM SYNTHESIS

PACS 43.90.+P; 73.40.Lq

The results of researches on the interaction of accelerated ions with a solid at the in situ ultrasonic treatment are reported. A proposed combined method of acoustically stimulated ion beam doping of solid-state targets allows one to efficiently control the redistribution of radiation-induced defects that emerge during the interaction of accelerated particles with the solid. This method makes it possible to affect the rate of quasichemical reactions in nano-sized structures, stimulate the acceleration or deceleration of mass transfer processes, and change conditions of formation, growth, and decay of phases in solid-state matrices.

K e y w o r d s: ion implantation, ultrasound excitation, defects, diffusion, nanoclusters, buried layers.

1. Introduction

The ion-stimulated processes of phase nucleation and formation in a solid run under nonequilibrium conditions and at a high concentration of radiation-induced defects [1, 2]. The high concentration of defects governs the character and the type of quasichemical reactions in the solid. New effective methods are needed to control the system of radiation-induced defects, which would make it possible to affect the technological processes of phase formation in nano-sized structures [3]. For this purpose, a combined method was proposed to control the system of radiation-induced defects in nano-sized surface layers by exciting a target with ultrasound (US) and simultaneously by irradiating it with a flux of accelerated ions [4].

Interaction of US waves with defects in an anisotropic semiconductor crystal has a complicated character, especially when point defects and acoustic waves are dynamically generated by an ion beam. In this case, the multiparticle interaction of US waves with plasmon, polariton, helicon, and other excitations of the crystal lattice takes place, and, as a result, there arise wave modes with various frequencies [5]. This should be taken into account, as well the fact that, in the course of implantation, there emerge metastable structural complexes, whose lifetime is comparable with the periods of US wave vibrations [6]. The action of US waves on such complexes can entail a local release of a considerable amount of energy, which would substantially accelerate the diffusion of impurities and defects.

A number of effects taking place, when this method was applied to the ion-beam synthesis of nanoclusters [7–9], buried dielectric layers [10, 11], oxidation of metallic films [12–14], amorphization of silicon surface layers [15–18], introduction of electrically active impurities [19–21], and relaxation of mechanical stresses in nano-sized thin-film systems [22], were studied. It should be noted that the effects concerned can be observed only if the process of ion implantation was carried out simultaneously with the US treatment of a target. The US treatment before or after the implantation did not invoke any of those effects and did not affect their magnitudes.

2. Experimental Technique

The introduction of US waves into a silicon wafer in the course of its acoustically stimulated ion-beam doping was provided, by using a specially developed specimen holder, the scheme of which is exhibited in Fig. 1. The voltage was supplied to the US transducer contacts from an HF generator, and its frequency was close to the resonance frequency of a transducer. On the working surface of a silicon wafer, an US detector was mounted. The signal from it was registered with the use of a spectrum analyzer. This allowed

us not only to optimize the conditions of the US introduction into a wafer from an HF generator, but also to monitor changes in the vibration spectrum and the generation of acoustic waves under the influence of an ion beam at the implantation. It was found that the US treatment manifests itself in the frequency interval from 0.7 to 9 MHz and at target excitation powers higher than 0.1 W/cm^2. The effects became stronger as the US treatment power increased. At the US treatment power higher than 1.5 W/cm^2, the intense heating of the target and the holder took place.

3. Experimental Results

3.1. Ion-beam amorphization of silicon at the ultrasonic matrix excitation

The amorphization of a surface layer, which accompanies the process of high-dose ion implantation, is widely used to reduce the channeling effect. It also plays an important role at the formation/redistribution of the depth distribution profiles of doping impurities during temperature-stimulated processes. Amorphization processes have also a fundamental interest for the radiation solid-state physics.

The influence of the US treatment on the amorphization of a silicon matrix at the implantation of argon ions was studied. In Fig. 2, the spectra of backward Rutherford scattering of ions for argon-implanted specimens subjected (curve *1*) and not subjected (curve *2*) to the US treatment in the course of implantation are depicted. For comparison, the spectrum of a reference (non-implanted) specimen (curve *3*) and the spectrum registered in the regime of arbitrary ion beam incidence (curve *4*) are also shown.

The peak width in those spectra characterizes the amorphous region thickness. One can see that the *in situ* US treatment considerably affects the structure (imperfection) of the near-surface region in single-crystalline silicon. In the absence of the US treatment, there is a layer (of about 28 nm) enriched with defects near the surface and an amorphous buried layer under it. The US treatment stimulates the formation of an amorphous layer immediately from the Si surface. In this case, the amorphous layer thickness is approximately 1.3 times as large.

3.2. Relaxation of mechanical stresses in SiGe films implanted with He^+ ions at the in situ ultrasonic treatment

We also studied two-component SiGe structures, which are known to be stressed in the initial state. Mechanical stresses in thin SiGe layers (80–150 nm) grown up on Si substrates can be relaxed by the implantation of H or He ions and by the thermal annealing [21]. However, the relaxation degree depends on technological regimes, and the process should be improved provided that the dislocation concentration is kept low. The relaxation degree in specimens at various fabrication stages of such structures can be determined from x-ray diffraction data.

In Fig. 3, the x-ray diffraction spectra obtained for 300-nm SiGe/Si specimens at various stages of their manufacture are shown. The arrows mark the positions of maxima for a completely relaxed (R) film and a coherently strained (S) one. The relaxation degree R was determined by the formula

$$R = \frac{a^{\top}_{\mathrm{SiGe}} - a_{\mathrm{Si}}}{a^{\parallel}_{\mathrm{SiGe}} - a_{\mathrm{Si}}} \times 100\%,$$

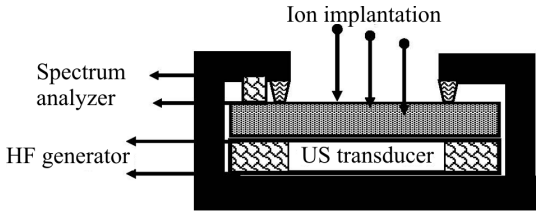

Fig. 1. Scheme of a holder for the *in situ* US treatment at the ion irradiation

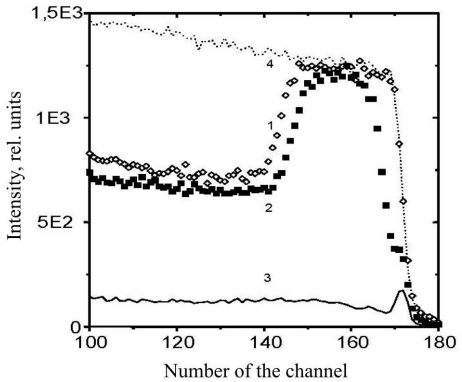

Fig. 2. Spectra of Rutherford back-scattering of ions for Si specimens: (*1*) implanted with Ar^+ ions (150 keV) with the US treatment, (*2*) implanted without the US treatment, (*3*) not implanted, and (*4*) an arbitrary spectrum

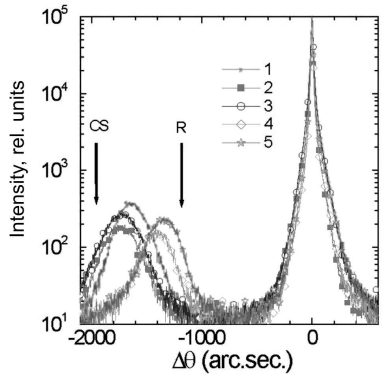

Fig. 3. X-ray diffraction curves for treated specimens: (*1*) initial, (*2*) after the implantation without US treatment, (*3*) after the implantation with the US treatment, (*4*) annealed after the implantation without US treatment, and (*5*) annealed after the implantation with the US treatment

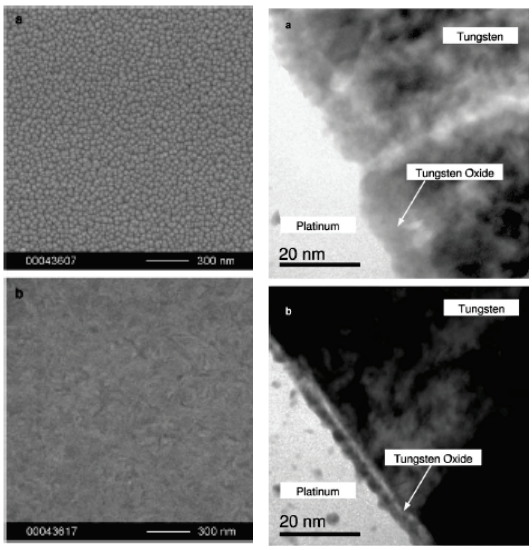

Fig. 4. TEM images of the tungsten oxide films: surfaces (right panels) and cross-sections (left panels): with (lower panels) and without (upper panels) the US treatment

where $a^{\top}_{\mathrm{SiGe}}$ and $a^{\parallel}_{\mathrm{SiGe}}$ are the lattice parameters of the SiGe layer measured perpendicularly and in parallel, respectively, to the surface, and a_{Si} is the lattice parameter of Si. The application of the US treatment allows the relaxation degree to be increased (curve *5*) at identical implantation doses and under identical annealing conditions. The maximum value of total R reaches 82% (much larger than without US treatment) for the specimens with a SiGe layer 300 nm in thickness at an US treatment power up to 1.5 W/cm^2.

3.3. Acoustically stimulated ion-plasma oxidation of tungsten films

Another task consisted in obtaining the thin layers of tungsten oxide with a sharp phase interface. A tungsten foil was subjected to the electro-chemico-mechanical polishing, which provided the surface roughness less than 2 nm. Oxidation was carried out in a reactive oxygen plasma at a power of 50 W and a working pressure of 0.5 Pa. US vibrations with a frequency of 5 MHz and a power of 1 W/cm^2 were excited in the film immediately during the oxidation. After the oxidation, the specimens were placed (not exposing them to air) to an analytical chamber for the researches using x-ray photoelectron spectroscopy (XPS) and mass spectroscopy.

The $4f$ peak of pure non-oxidized tungsten is a doublet consisting of a component with a binding energy of 31.15 eV for W $4f_{7/2}$ and another component shifted by 2.15 eV and resulting from the spin-orbit splitting. The exposure of the tungsten surface in an oxygen plasma gives rise to the surface oxidation and the appearance of the second doublet peak with a binding energy of 35.28 eV for W $4f_{7/2}$ and the spin-orbit splitting shifted by 2.14 eV. This doublet corresponds to the oxidized state W^{6+}, and the increase of the expose time in plasma makes its intensity higher and reduces the intensity of the former doublet (at 31.15 eV). The intensity growth for the doublet associated with the oxidized state (at about 36 eV) and the intensity reduction for the doublet associated with the metallic state (at 31.15 eV) are more rapid if the oxidation is carried out without US treatment. In other words, the ion-plasma oxidation of the tungsten surface simultaneously with the US treatment provides the formation of a thin dense layer of tungsten oxide, which is characterized by a low content of voids. The internal interface WO_2/W at the oxidation with the US treatment is very sharp in comparison with the ordinary plasma oxidation.

Electron microscopy images (Fig. 4) confirm a conclusion based on the results presented above concerning the formation of a thin (about 5 nm) dense tungsten oxide film under the US treatment conditions (panel *b*) in contrast to a porous film formed under conditions of the ordinary plasma oxidation (panel *a*).

In Fig. 5, the results of level-by-level secondary ion mass spectrometry (SIMS) analysis of specimens after their exposure in a plasma for 3600 s are shown. One can see that the distribution profile of the tungsten oxide phase (the WO_3 signal) in the specimens subjected to the US treatment has a sharp recession at a depth of 5–6 nm, whereas a smooth intensity recession to a depth of more than 10 nm is observed in the specimens not subjected to US treatment. Such a behavior of the signal agrees with the XPS data testifying to a different thickness of the near-surface tungsten oxide layer. The depth distributions of the OH^- signal also essentially differ for those specimens. A high intensity of the OH^--ion yield is inherent to porous and friable targets. The level of this signal in the specimen subjected to the US treatment is 10 times lower.

3.4. Peculiarities of the ion-beam formation of metal nanoclusters in silicon dioxide at the ultrasonic excitation of a substrate

This section concerns the researches dealing with the mechanisms of nanocluster formation under the action of ultrasound. A series of experiments on the ion-beam synthesis of metal (copper, silver) nanoclusters in SiO_2 matrices were carried out. As a stimulating factor for the nucleation and the accelerated growth of such clusters, the *in situ* US treatment of the substrate was used.

For implanted metal ions, the probability of their oxidation or the silicide formation is high. Therefore, for the formation of metal nanoclusters in the silicon dioxide matrix to be efficient, it is necessary to provide conditions, under which the rates of oxidation and silicide formation are minimized, but the process of metal-atom clustering remains sufficiently rapid. Such conditions can be realized (i) at rather low temperatures after the implantation annealing in order to decelerate the silicide formation and (ii) at high concentration of defects of the vacancy type in the cluster formation region in order to accelerate the cluster nucleation and growth.

Copper ions $^{63}Cu^+$ with an energy of 50 keV were implanted into a SiO_2 film 100 nm in thickness to a dose within the interval of $(1 \div 5) \times 10^{15}$ cm^{-2}. Some of the specimens were implanted under US treatment conditions (9 MHz, the US power varied from 0.1 to 0.5 W/ cm^2).

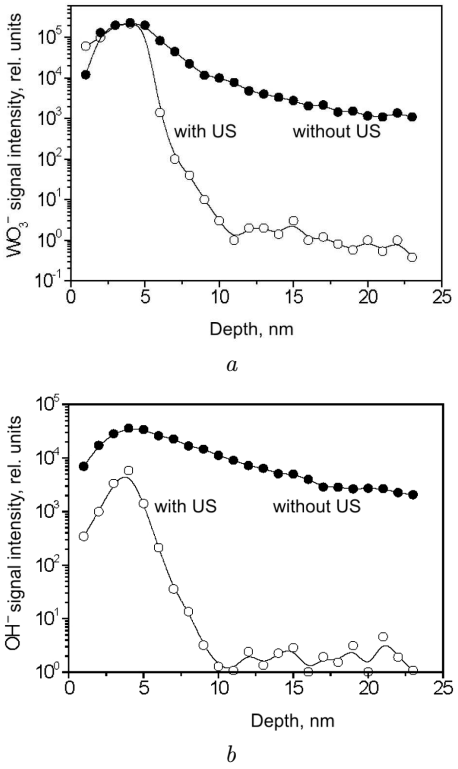

Fig. 5. SIMS profiles for the intensity distribution of the WO_3^-- (*a*) and OH^+- (*b*) ion yields over the specimen depth after the 3600-s exposure in an oxygen plasma

In the specimens not subjected to the US treatment, there were no nanoclusters, and the process of copper nucleation took place only provided the excess of vacancies (under US treatment). The formation of copper nanoclusters in specimens not subjected to the US treatment started only at an implantation dose of 2.5×10^{15} cm^{-2}.

If the copper concentration was five times as high (at an implantation dose of 5×10^{15} cm^{-2}), copper precipitates were actively formed irrespective of whether the implantation was carried out with the US treatment or not (see Fig. 6). One can see that the dimensions of nanoclusters reach a value of 5–6 nm in the case of acoustically stimulated synthesis (panel *a*) and only 2.5 nm at ordinary implantation (panel *b*).

Silver ions $^{108}Ag^+$ with an energy of 40 keV were implanted into a thermally grown SiO_2 film 100 nm in thickness to a dose of 3×10^{15} cm^{-2}. Some of the specimens were implanted under the *in situ* US treatment conditions (5 MHz, the US power varied from

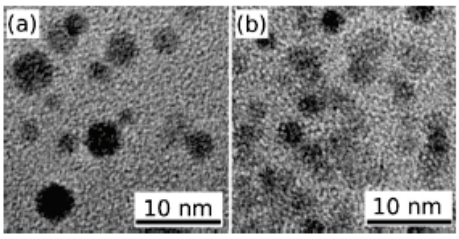

Fig. 6. TEM images of copper clusters in the SiO_2 film synthesized by implanting $^{63}Cu^+$ ions to the dose $D_{Cu} = 5 \times 10^{15}$ cm^{-2}: implantation (a) with and (b) without US treatment

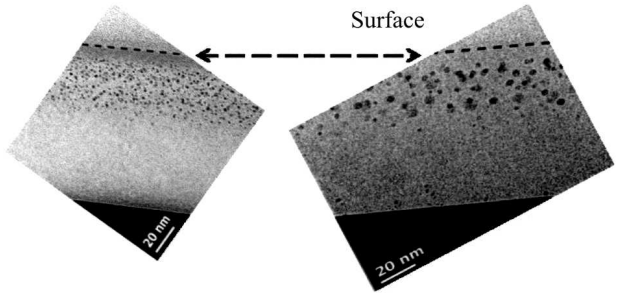

Fig. 7. TEM images of SiO_2 films with silver nanoclusters formed by the ion implantation: (a) without and (b) with *in situ* US treatment

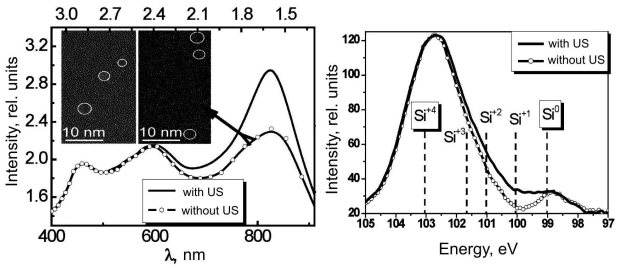

Fig. 8. (a) PL spectra and (b) XPS data for structures with nc-Si obtained using the ion implantation method

Relative integral intensities of oxidized silicon states

	Si^0	Si^{1+}	Si^{2+}	Si^{3+}	Si^{4+}
With US	9.48%	1%	0%	0%	89.52%
Without US	9.6%	3.27	1.55%	6.25	79.33%

0.1 to 0.5 W/ cm^2). After the implantation, the specimens were annealed in vacuum at a temperature of 550 °C for 20 min. In Fig. 7, the transmission electron microscopy (TEM) images of a silicon dioxide film with silver clusters formed during the annealing are shown.

As was in the case where copper clusters were synthesized (Fig. 6), the size of silver precipitates formed during the thermal annealing is much bigger in the case of acoustically stimulated ion-beam synthesis. The average size of nanoclusters amounted to 1.9 ± 0.35 nm for specimens implanted without US treatment and to 3.4 ± 0.65 nm if the US treatment was applied. Those results comprise a direct proof that the growth of nanoclusters can be stimulated by applying a combined (US + implantation) treatment.

3.5. Photoluminescence of structures with Si nanoclusters obtained by the acoustically stimulated ion implantation

The size of silicon nanoclusters formed in the SiO_2 matrix by implanting silicon ions to high doses weakly depends on the intensity and the frequency of the US treatment. The TEM data confirm the formation of an array of nanoclusters with approximately identical dimensions and characterized by a practically uniform concentration both at the ordinary implantation and at the implantation with the US treatment (see the inset in Fig. 8, a). However, the corresponding photoluminescence (PL) spectra have substantial differences.

According to work [23], the PL band at 1.5–1.6 eV can also be connected with the recombination through the electron states at the nanocluster interfaces Si–SiO_2. Therefore, in order to discriminate possible mechanisms of US treatment influence on the PL intensity, we studied x-ray photoelectron spectra of those structures (Fig. 11, b). The resolution of x-ray photoelectronic spectra into elementary components in accordance with the method described in work [9] gave us five elementary components in the Si-2p spectrum, which correspond to different degrees of oxidation of silicon in the matrix (i.e. to different Si_nO_m clusters). In Table, the calculated relative integral intensities of silicon oxidation states are shown. The component Si^0 corresponds to non-oxidized silicon (nanoclusters), Si^4 to completely oxidized silicon (the SiO_2 matrix), and the other components to intermediate oxidized states.

The XPS data show that, if the US treatment is applied, the formed interface Si-nc/SiO_2 is more per-

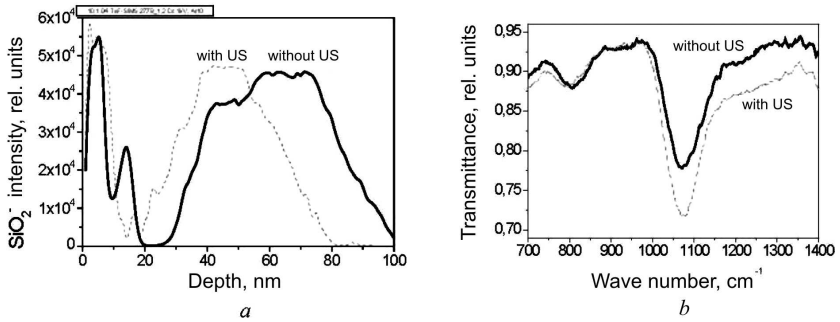

a *b*

Fig. 9. (*a*) SIMS profiles of oxygen distribution and (*b*) IR absorption spectra in structures with a buried SiO_2 layer

fect (single-, double-, and triple-oxidized silicon is practically absent). Just in this case, a substantial reduction in the PL band intensity with a maximum at 800 nm is observed, i.e. a decrease of the "transient" SiO_x suboxide layer at the interface between the nanocluster and the SiO_2 matrix is accompanied by a PL reduction. The intensity of the PL band at 800 nm and the total concentration of suboxide states decrease, as the US treatment power increases.

Taking into account that the average size of Si nanoclusters and their size distribution are not practically changed at the US treatment, the similar character of the dependences of the PL intensity and the concentration of suboxide states on the power of applied US waves testifies that the band at 800 nm is associated with suboxide states at the interface nc-Si/SiO_2.

3.6. Ultrasound effect on the formation of silicon-on-insulator structures

Another structure actual for microelectronics is the structure with a buried dielectric layer. When buried dielectric layers are ion-beam synthesized by means of the high-dose oxygen implantation into a silicon wafer, the ultrasonic excitation efficiently affects only the nucleation of the dielectric phase at initial annealing stages. This fact is related to a high vacancy concentration in the near-surface region, so that the process of oxidation and filling of all vacancy complexes runs very quickly (within several minutes).

In order to elucidate the influence of the acoustically stimulated implantation on the processes of ion-beam formation of the buried oxide and silicon nitride layers, the following experiments were carried out. For the formation of buried layers, N_2^+ or O_2^+ ions with an energy of 65 keV were implanted to a dose of 1×10^{17} cm^{-2}. Ultrasound vibrations with a frequency of 2 MHz were generated in the wafers. After the implantation, the specimens were annealed in the Ar environment in the temperature interval of 1000–1200 °C.

Impurity distribution profiles were studied using the method of time-of-flight secondary ion mass spectrometry (TOF-SIMS IV) in the regime of target sputtering with Cs^+ ions at an energy of 0.5 keV and Ar^+ ones at an energy of 10 keV for the secondary-ion generation. We also considered the spectra of the infra-red transmission in order to analyze the structure and the composition of the embedded dielectric layer. The distribution profiles of oxygen in the specimens after the oxygen implantation and the annealing are exhibited in Fig. 9. One can see from the figure that an appreciable shift of the oxygen distribution profile (the dotted curve) toward the surface and an increase of the concentration maximum (the signal intensity is almost the same as for the SiO_2 phase) are observed for specimens implanted simultaneously with the *in situ* US treatment. The IR absorption spectra also demonstrate the more efficient light absorption stemming from a higher content of the silicon oxide phase in the specimens subjected to the US treatment. In the case of the nitrogen implantation, variations in the distribution profiles are insignificant, although the specimens with the US treatment reveal a certain displacement of the profiles toward the surface.

Hence, the application of the US treatment at the synthesis of buried silicon dioxide layers is expedient to be used, provided that the oxygen concentration is relatively low (below the SiO_2 stoichiometry), for the creation of phase nucleation regions and/or for

the controllable diffusion-driven displacement of an implanted impurity.

Therefore, the *in situ* US treatment alone cannot be a method that improves the quality of buried dielectric layers. It is so because the rapid growth of precipitates under the conditions, when the concentrations of oxygen and vacancies are high, can stimulate a covering of separate silicon islands with large dimensions by a continuous SiO_2 layer. Afterward, such silicon inclusions cannot be oxidized owing to a low permeability of the film that covers them.

4. Discussion of the Model and the Mechanisms of Acoustically Stimulated Implantation

The efficiency of the US treatment is associated with the fact that, in the case of ultrasound action, the high-intensity fluxes of phonons are realized in the excited medium even at relatively small vibration amplitudes [24]. Really, the average density of mechanical energy $E_{\rm us}$ transferred by the acoustic wave to a certain volume of the solid,

$$E_{\rm us} = \frac{1}{2}\rho\omega_{\rm us}^2 U_{\rm oi}^2,$$

where ρ is the solid density, U_{oi} the deformation, and $\omega_{\rm us}$ the frequency of ultrasound wave, grows quadratically with the US wave frequency. This circumstance easily provides the emergence of various nonlinear processes resulting in the intense defect formation (or, on the contrary, in the defect annihilation) at places of a weakened lattice: dislocations, clusters, artificially created layers (as in the case of ion implantation) enriched with point defects, and others. A decrease of the local solid density and the thermodynamic potential results in a threshold reduction for the structural transformations in this region (ordering, induced diffusion, generation of higher-frequency US waves owing to system's nonlinearity). The nonlinearity of the energy absorption, which may appear as the amplitude of US waves increases, results in the invoking of additional effects, in particular, the emergence of a powerful pulse shock wave, the absorption of which by radiation-induced defects is anomalously high.

Let us concentrate attention on the effect of point-defect redistribution by US waves, which was observed in the described experiments. In the case of implantation without US treatment, the localization regions of vacancies, interstitial atoms, and implanted impurities practically coincide. At the US treatment, the recoil atoms generated when the accelerated particle interacts with the surface layer are in the field of sign-alternating mechanical stresses: there emerge tensile and compressed regions in the target depth. For an interstitial silicon atom (Si_i) or a recoil atom with a kinetic energy sufficient to overcome interatomic potential barriers, the conditions for their motion into the wafer depth are created, when a stretched region appears. The depth of a Si_i displacement as a result of its multiple collisions under the US treatment conditions can reach considerable values (up to several hundred nanometers). Under those conditions, the probability of the annihilation of the complexes vacancy-Si_i decreases, and vacancies are accumulated in the near-surface region [17,18]. When tensile stresses take place in the near-surface region, one may expect a coagulation of vacancies into vacancy complexes. This process can occur in the cases where the number of vacancies is large, and those vacancies, which are intensively accumulated during the implantation in the course of the US treatment, minimize their surface energy by assembling into vacancy complexes.

After the implantation process has terminated, the depth distribution of radiation-induced defects has substantial differences between the cases of ordinary implantation (Fig. 10, *d*) and implantation with the US treatment (Fig. 10, *b*). In the specimens implanted with the US treatment, the surface layer is saturated with vacancies, the layer with the implanted impurity is located more deeply, and even more deeply is located the layer with interstitial silicon atoms. This situation is unique from the viewpoint of the creation of conditions for the controllable formation or modification of nano-size near-surface layers and their parameters, i.e. for the development of a new technique of acoustically stimulated implantation of ions. The formation of a near-surface region enriched with vacancies and the displacement of interstitial atoms into the depth can accelerate the processes of nanocluster nucleation and growth at the annealing, diminish the undesirable radiation-enhanced diffusion of impurities, favor the thermal activation of electrically active impurities, and affect the distribution and the relaxation of mechanical stresses in layered structures.

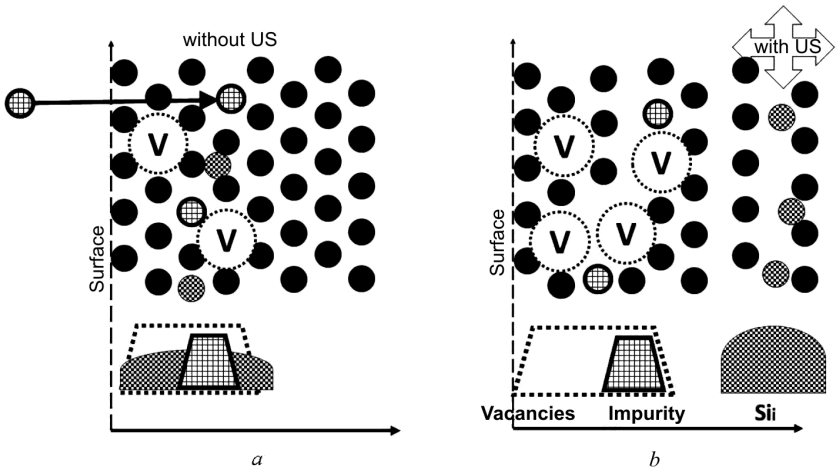

Fig. 10. Distributions of radiation-induced defects after the implantation (*a*) without and (*b*) with the *in situ* US treatment

In order to establish how the US treatment influences the diffusion of interstitial atoms and whether a vacancy-enriched region is really formed at the ion implantation into an amorphous SiO_2 film, the following experiments were carried out [8].

4.1. Treatment of implanted structures in a deuterium plasma

A SiO_2 film 100 nm in thickness located on a Si wafer of boron doped (100) grade was implanted with 40-keV Ar^+ ions to a dose of 1×10^{14} cm^{-2}. For some specimens, the *in situ* US treatment conditions (9 MHz, 1 W/cm^2) were realized. After the implantation, the specimens were treated in a deuterium plasma (200 °C, 30 W, 0.02 mbar, 40 min) in order to cover the regions with the increased concentration of vacancies.

In Fig. 11, the profiles of deuterium concentration distribution (the D_2 signal) over the depth of specimens after their treatment in a deuterium plasma are depicted. They were obtained using the secondary ion mass spectrometry (SIMS) method. One can see from the figure that, in the specimens implanted under the US treatment conditions (curves *2* and *3*), the deuterium concentration in the SiO_2 film is several times higher in comparison with that in the specimen without US treatment (curve *1*). The amount of accumulated deuterium is proportional to the vacancy concentration and, as curves *2* and *3* testify, increases, when the ultrasonic excitation intensity grows. Deuterium is also accumulated at the internal

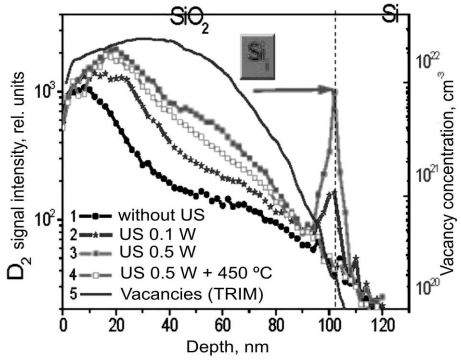

Fig. 11. Profiles of the deuterium concentration distribution (D_2 signal) for argon-implanted specimens: (*1*) without US treatment; (*2*) US treatment at 0.1 W/cm^2, (*3*) US treatment at 0.5 W/cm^2, (*4*) US treatment at 0.5 W/cm^2 + annealing at 450 °C, (*5*) vacancy distribution (SRIM calculation)

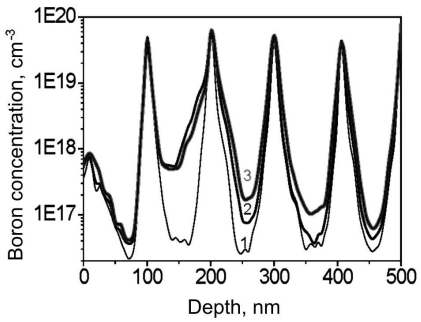

Fig. 12. SIMS profiles of the boron distribution after the implantation of Si^+ ions (*1*) and the annealing in the structure with δ-doped boron layers: (*2*) without and (*3*) with the US treatment

interface SiO_2/Si. At the implantation with the US treatment, a considerable number of both vacancies and interstitial atoms are generated. Hydrogen/deuterium decorates defects of different types with different efficiencies (vacancies are decorated the most efficiently). Therefore, in order to establish the dominating type of defects in the SiO_2 film, the specimens, after the plasma treatment, were annealed in an inert atmosphere at a temperature of 450 °C. Under such annealing conditions, an active mutual annihilation of vacancies and interstitial atoms takes place, and, in the case where their local concentrations are identical (the case of the implantation without US treatment), the film completely restores its structure, and deuterons escape from it. The figure also demonstrates that, after the annealing (curve *4*), the deuterium concentration (in the specimens with the US treatment) remains high in the region of the radiation-induced defect distribution. In other words, after the annihilation of radiation-induced defects, the region enriched with vacancies survives.

4.2. Diffusion of boron atoms implanted in silicon

According to the proposed model, in the case of implantation with the US treatment, a spatial separation of point defects takes place: vacancies are located near the surface, and interstitial defects diffuse into the crystal depth. In order to study the effects of redistribution of radiation-induced defects (Si_i), we fabricated test specimens with δ-doped boron layers in silicon (10 δ-layers). The smearing of the latter at the annealing should testify to an excess concentration of Si_i. The effect of enhanced boron diffusion is known to manifest itself in regions with an excess of interstitial silicon atoms.

In Fig. 12, the profiles of boron distribution in structures with δ-doped layers after their implantation with silicon ions and the annealing at a temperature of 950 °C are depicted. Besides the active smearing of the second-layer region (the region of Si^+ implantation), the third and (partially) fourth δ-doped layers become appreciably smeared. This smearing (layers 3 and 4) is much more intense in the specimen implanted with the US treatment (curve *3*), which testifies to the presence of excess interstitial silicon in those regions. In other words, we may assert that it was the US treatment at the ion implantation that stimulated Si_i to move into the specimen bulk by several hundred nanometers. In the specimens implanted with the US treatment, the observed broadening of deep δ-layers is much stronger, which testifies to the accelerated diffusion of Si_i into the bulk.

5. Conclusions

A new method of acoustically stimulated ion-beam doping (synthesis) of solid-state specimens has been proposed. The method allows one to efficiently control the redistribution of radiation-induced defects generated during the interaction between accelerated particles and the solid. The following effects resulting from this interaction under the *in situ* US treatment were revealed.

- Accelerated amorphization of surface layers in single-crystalline silicon under the action of irradiation with argon and boron ions.
- A reduction of the influence of radiation-induced defects on the accelerated diffusion (its deceleration) of implanted boron by reducing the number of interstitial silicon atoms in the region of the implanted boron distribution.
- An increase of the relaxation degree of mechanical stresses in SiGe surface films deposited on the silicon surface by 5–6% at the implantation of He ions.
- Accelerated formation of dense surface WO_3 films with a sharp (a transient layer of about 1 nm) interface film/substrate at the ion-plasma oxidation of tungsten.
- Accelerated nucleation and growth of metal (Cu, Ag) and semiconductor (Si) nanoclusters at their ion-beam synthesis in the SiO_2 matrix; a modification of the interface nc-Si/SiO_2 and the increase of the average size of metal clusters by almost a factor of two.

The work was sponsored by the Ministry of Science and Education of Ukraine (grants Nos. M/175-2007, M/90-2010, and M/212-2011) in the framework of Interdepartmental scientific and engineering program "Nanophysics and nanoelectronics" headed by Academician of the NAS of Ukraine M.G. Nakhodkin. The authors are grateful to him for his permanent attention and valuable advice. We also express our gratitude to our collaborators and colleagues V.G. Popov, V.P. Klad'ko, and O.S. Oberemok for their assistance during this work.

1. J.F. Ziegler, *Ion Implantation: Science and Technology* (Academic Press, San Diego, 1988).
2. M. Nastasi and J.W. Mayer, *Ion Implantation and Synthesis of Materials* (Springer, Berlin, 2006).
3. O. Bondarchuk, S. Goysa, I. Koval, P. Melnik, and M. Nakhodkin, Appl. Surf. Sci. **255**, 6421, (2009).
4. D. Krueger, R. Kurps, B. Romanjuk, V. Melnik, and Ja. Olich, Patent US 6358823 B1 (2002).
5. B. Lüthi, P*hysical Acoustics in the Solid State* (Springer, New York, 2007).
6. A.G. Chelyadinsky and F.F. Komarov, Usp. Fiz. Nauk **173**, 813 (2003).
7. A. Romanyuk, V. Spassov, and V. Melnik, J. Appl. Phys. **99**, 034314 (2006).
8. A. Romanyuk, P. Oelhafen, R. Kurps, and V. Melnik, Appl. Phys. Lett. **90**, 013118 (2007).
9. A. Romanyuk, V. Melnik, Ya. Olikh, J. Biskupek, U. Kaiser, M. Feneberg, K. Thonke, and P. Oelhafen, J. Luminesc. **130**, 87 (2010).
10. V.G. Litovchenko, A.A. Efremov, B.N. Romanyuk, V.P. Mel'nik, and C. Claeys, J. Electrochem. Soc. **145**, 8 (1998).
11. V. Litovchenko, B. Romanyuk, V. Melnik, V. Klad'ko, V. Popov, O. Oberemok, and I. Khatsevich, Solid State Phenom. **178**–**179**, 17 (2011).
12. A. Romanyuk, P. Oelhafen, R. Steiner, P.M. Nellen, J.C. Reiner, and V. Melnik, Surf. Sci. **595**, 35 (2005).
13. A. Romanyuk, R. Steiner, V. Melnik, and V. Thommen, Surf. Interf. Anal. **38**, 1242 (2006).
14. A. Romanjuk, V. Melnik, and P. Oelhafen, Nucl. Instrum. Methods Phys. Res. B **232**, 358 (2005).
15. B. Romanyuk, D. Krüger, V. Melnik, V. Popov, E. Borshchagovskyi, Ya. Olikh, and V. Soroka, Ukr. J. Phys. **46**, 191 (2001).
16. B. Romanyuk, V. Melnik, Ya. Olikh, V. Popov, and D. Krüger, Semicond. Sci. Technol. **16**, 397 (2001).
17. M.G. Nakhodkin and M.I. Fedorchenko, Metallofiz. Noveish. Tekhnol. **26**, 1639 (2004).
18. N. Nakhodkin, N. Kulish, and T. Rodionova, Phys. Status Solidi A **207**, 316, (2010).
19. D. Krüger, R. Kurps, B. Romanyuk, V. Melnik, and Ya. Olikh, J. Vac. Sci. Technol. B **20**, 1448 (2002).
20. V.P. Melnik, Y.M. Olikh, V.G. Popov, B.M. Romanyuk, Y.V. Goltvyanskii, and A.A. Evtukh, Mater. Sci. Eng. B **124**–**125**, 327 (2005).
21. O.I. Gudimenko, V.P. Kladko, V.P. Melnik, Ya.M. Olikh, V.G. Popov, B.M. Romanyuk, M.V. Slobodian, and P.P. Kogutyk, Ukr. J. Phys. **53**, 140 (2008).
22. B.M. Romanjuk, V.P. Kladko, V.P. Melnik, V.G. Popov, V.M. Yuchimchuk, A.I. Gudymenko, Ya.M. Olikh, G. Weidner, and D. Kruger, Mater. Sci. Semicond. Process. **8**, 171 (2005).
23. C. Ternon, F. Gourbilleau, C. Dufour, J.L. Doualan, and B. Garrido, J. Luminesc. **99**, 361 (2002).
24. V.A. Krasilnikov and V.V. Krylov, *Introduction to Physical Acoustics* (Nauka, Moscow, 1984) (in Russian).

Received 22.10.14.
Translated from Ukrainian by O.I. Voitenko

В.Г. Литовченко, В.П. Мельник, Б.М. Романюк

ФОРМУВАННЯ НАНОРОЗМІРНИХ ФАЗ ПРИ АКУСТО-СТИМУЛЬОВАНОМУ ІОННО-ПРОМЕНЕВОМУ СИНТЕЗІ

Р е з ю м е

Представлено результати досліджень взаємодії прискорених іонів з твердим тілом при *in situ* ультразвуковій обробці. Запропонований комбінований метод акусто-стимульованого іонно-променевого легування (синтезу) твердотільних мішеней дозволяє ефективно управляти перерозподілом радіаційних дефектів, які виникають під час взаємодії прискорених частинок з твердим тілом. Використання цього методу дозволяє впливати на швидкість протікання квазіхімічних реакцій в нанорозмірних структурах, стимулювати прискорення або уповільнення процесів масопереносу і змінювати умови формування, росту або розпаду фаз у твердотільних матрицях.